Deriving a Soil Loss Equation for Sediment Yield Estimation

Manaye Getu Tsige[1,2*] and Andreas Malcherek[1]

[1] *Department of Civil Engineering and Environmental Sciences, Universität der Bundeswehr München, 85579, Neubiberg, Germany*
[2] *Department of Water Resources Engineering, Adama Science and Technology University, 1888, Adama, Ethiopia*

*Corresponding Author: Manaye Getu Tsige; manaye.tsige@unibw.de,

manaye.getu@astu.edu.et

Abstract

The Modified Universal Soil Loss Equation (MUSLE) is one of the commonly used empirical soil erosion models for the estimation of the amount of soil loss from the area of a catchment. Different improved versions of the MUSLE are available. However, in the MUSLE and improved versions of the MUSLE, the effect of topography and the relationship between soil erodibility and runoff on soil erosion and sediment transport are not explicitly explained.The MUSLE and other similar soil erosion models had been developed on the basis of regression analysis, and mathematical or physical interpretation. They do not provide a detailed physical explanation of soil erosion and sediment transport. Therefore, deriving a physically based soil loss equation for sediment yield estimation (SLESYE) becomes important to explain the aforementioned problems. To derive the equation, we considered the potential energy of runoff, the kinetic energy of rainfall, work done by runoff volume, and soil shear resistance. Physically speaking, the SLESYE is the most appropriate than the MUSLE and improved ver-

sions of the MUSLE, and it is also advantageous to the data-scarce area. Moreover, the SLESYE showed the best performance compared with the MUSLE and an improved MUSLE for all four watersheds under our consideration.

Keywords: soil erosion, sediment transport, sediment yield, erosion models

0.1. Introduction

The most commonly used lumped empirical soil erosion models are the Universal Soil Loss Equation (USLE) [Wischmeier and Smith, 1978], Revised Universal Soil Loss Equation (RUSLE) [Renard et al., 1997] and Modified Universal Soil Loss Equation (MUSLE)[Williams, 1975, 1977]. The other similar soil erosion models are the USLE-M [Kinnell and Risse, 1998], Chines Soil Loss Equation (CSLE) [Baoyuan et al., 2002], USLE-MM [Bagarello et al., 2015], USLE-MB [Bagarello et al., 2018], improved MUSLE which does not consider the peak runoff rate [Tsige et al., 2022a], improved MUSLE which considers the peak runoff rate [Shi et al., 2022], and a modified RUSLE [Gao et al., 2024].

Williams (1975) developed the MUSLE using 778 storm runoff events collected from 18 small watersheds [Williams, 1975, 1977], with areas varying from 15 to 1500 ha, slopes from 0.9 to 5.9%, and slope lengths of 78.64–173.74 m (Hann et al. 1994), as cited in [Sadeghi et al., 2014]. The MUSLE is given by

$$y = a(Qq)^b KLSCP$$

where y is the sediment yield in metric tons, a is the coefficient, b is the exponent ($a = 11.8$ and $b = 0.56$ for USA, where the MUSLE was originally

developed), Q is the runoff volume in m^3, q is the peak runoff rate in $m^3 s^{-1}$, K is the soil erodibility factor in $0.01 * tons * acre * hour * acre^{-1} * year^{-1} * foot^{-1} * tons^{-1} * inch^{-1}$, L is the slope length factor, S is the slope steepness factor, C is the cover factor, and P is the soil conservation practice factor.

The above soil erosion models had been developed on the basis of regression analysis, and mathematical or physical interpretation. They do not provide a detailed physical explanation of soil erosion and sediment transport. In the MUSLE and improved versions of the MUSLE, the effect of the topographic factor on soil erosion and sediment transport is not clear (for explanations, refer to Tsige et al. [2022b,a]). Also, the relationship between soil erodibility and runoff on soil erosion and sediment transport is not explicitly explained. Therefore, deriving a physically based soil loss equation for sediment yield estimation(SLESYE) becomes important to explain the aforementioned problems. To derive the equation, we considered the potential energy of runoff, the kinetic energy of rainfall, work done by runoff volume, and soil shear resistance.

We evaluated the SLESYE at four watersheds of Ethiopia, and we checked whether the SLESYE was better at estimating sediment yield than the MUSLE or improved MUSLE. We briefly discussed and compared the SLESYE against MUSLE or improved MUSLE based on physical concepts associated with soil erosion and sediment transport.

0.2. Materials and Methods

0.2.1. Description of Study Areas

For our study, we considered four watersheds in Ethiopia such as the Gumera Watershed, Gilgel Gibe 1 Watershed, Hombole and Mojo watersheds as shown in figure 1.

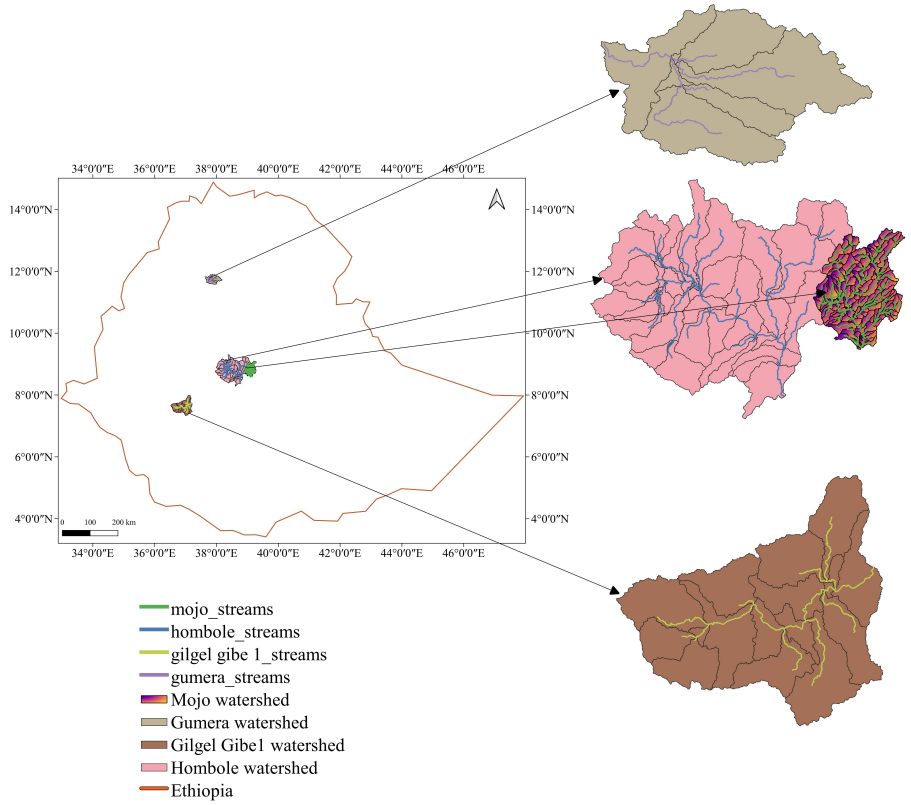

Figure 1: Location of four watersheds under our consideration.

We described the hydroclimate, land use, and soil of the study areas based on the data, which were prepared or obtained from different sources. Therefore, our description of the study area was based on climatic data which were ob-

tained from the National Meteorology Agency of Ethiopia, flow and sediment data which were obtained from the River Basin Authority of Ethiopia, and soil maps and land use maps which were prepared from different sources (land use and soil maps from the River Basin Authority of Ethiopia, harmonized world soil data, field observation report from the International Soil Reference and Information Centre, Global land service map, and historical imagery in the Google Earth Pro) by comparative and logical approaches.

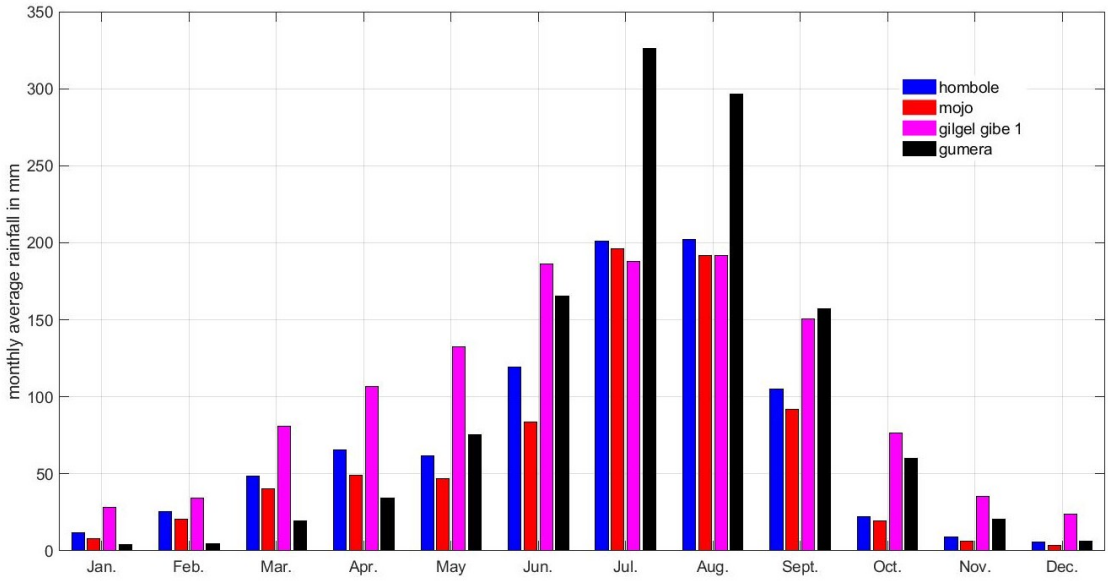

Figure 2: Monthly average rainfall of each watershed under consideration.

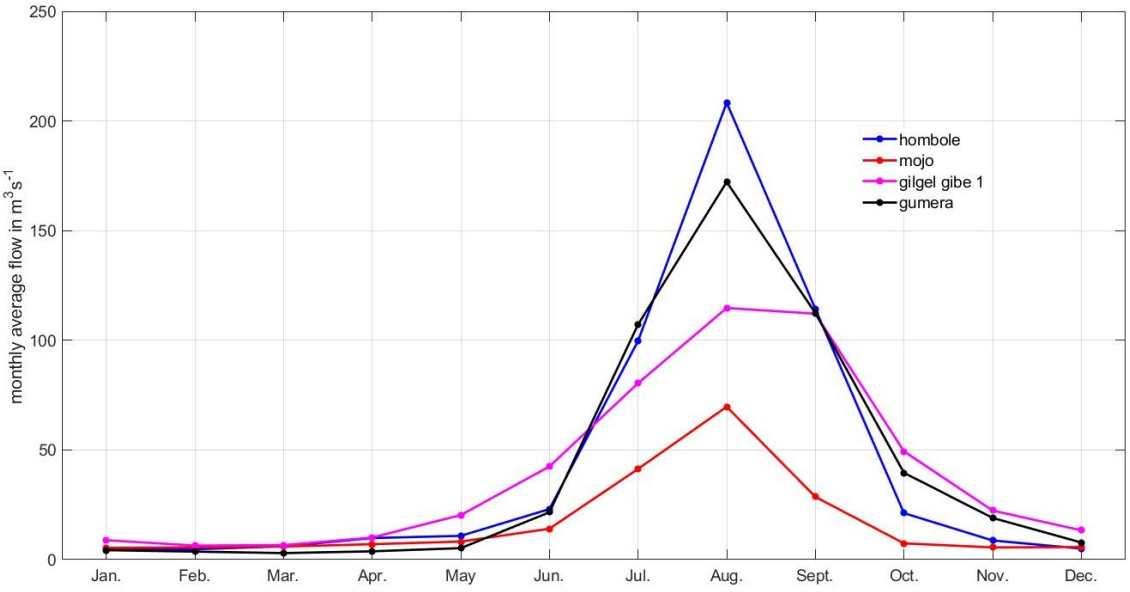

Figure 3: Monthly average flow at the main outlet point of each watershed under consideration.

0.2.1.1. Upper Awash River Basin

The Upper Awash River Basin drains into the Koka hydroelectric power reservoir. The basin comprises two main gauged watersheds: the Hombole and Mojo watersheds, which cover 65.26% and 12.87% of the total area of the basin, respectively. The basin also includes an ungauged watershed which covers 21.87% of the total area of the basin. The total drainage area of the basin is estimated to be 11,680.25 km^2.

For the Hombole and Mojo watersheds (see figure 1), the monthly average rainfall and monthly average flow at the main outlet points of the watersheds are given in figures 2 and 3, respectively. The average of suspended sediment concentrations recorded within the record period from 1989 to 2015 at the main outlet points of the Hombole and Mojo watersheds was 1.5 kg/m^3 and 0.16

kg/m^3 respectively. The annual average maximum and minimum temperatures were 25.56 °C and 10.06 °C, respectively. Land use change has been observed in the watershed as shown in figure A.1 – A.4. However, the dominant land use class of the watersheds is agricultural land. The dominant soil types are given in figure 4.

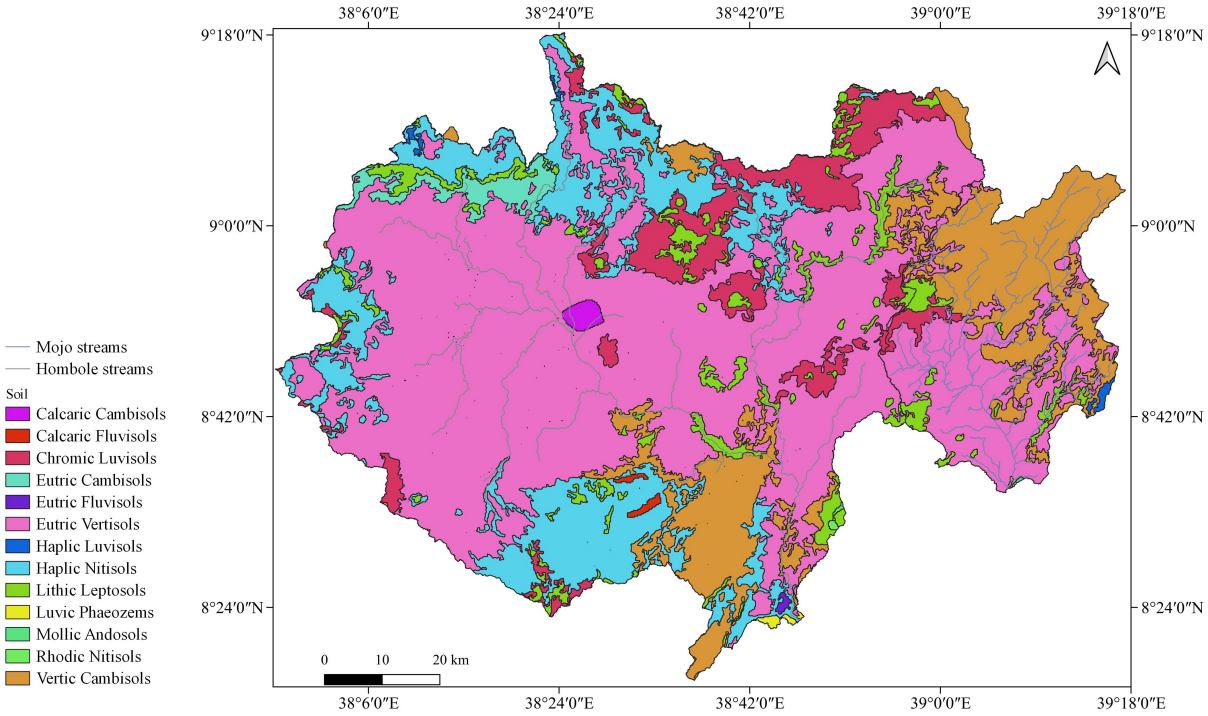

Figure 4: Soil maps of the Hombole and Mojo Watersheds.

0.2.1.2. Gumera Watershed

The Gumera Watershed drains into Lake Tana. Its geographic boundary is given in figure 1. The total drainage area of the watershed is estimated to be 1278.05 km^2.

The monthly average rainfall and monthly average flow at the main outlet

point of the watershed are given in figures 2 and 3, respectively. The average of suspended sediment concentrations recorded within the record period from 1990 to 2017 at the main outlet point of the watershed was 3.43kg/m^3. The annual average maximum and minimum temperatures were 25.38 °C and 10.02 °C, respectively. Land use change has been observed in the watershed as shown in figure A.5 and A.6. However, the dominant land use class of the watershed is agricultural land. The dominant soil types are given in figure 5.

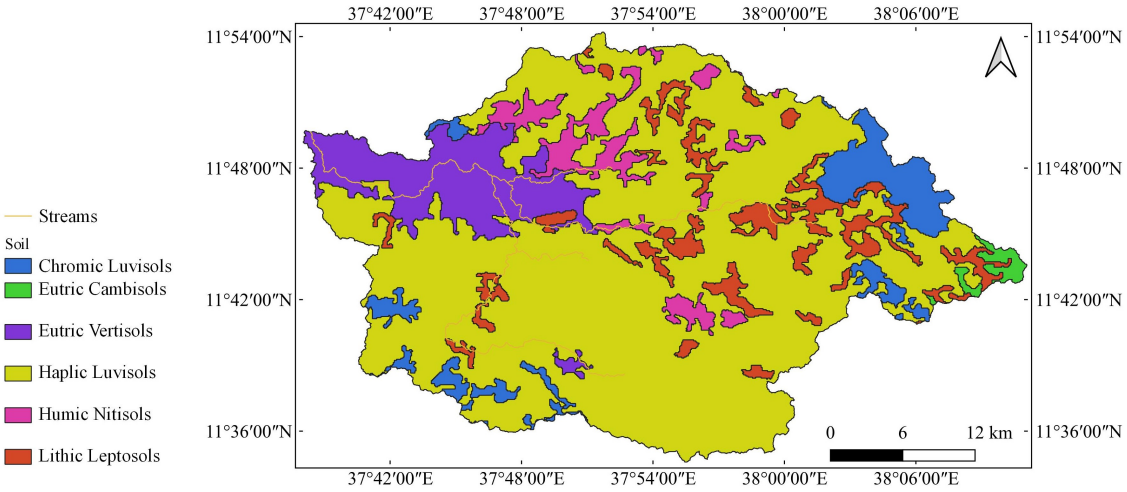

Figure 5: Soil map of the Gumera Watershed.

0.2.1.3. Gilgel Gibe 1 Watershed

The Gilgel Gibe 1 Watershed drains into the Gilgel Gibe 1 hydroelectric power reservoir. Its geographic boundary is given in figure 1. The total drainage area of the watershed is estimated to be 2928.09 km^2.

The monthly average rainfall and monthly average flow at the main outlet point of the watershed are given in figures 2 and 3, respectively. The average of suspended sediment concentrations recorded within the record period from

1990 to 2017 at the main outlet point of the watershed was 0.43 kg/m^3. The annual average maximum and minimum temperatures were 25.36 °C and 11.7 °C, respectively. Land use change has been observed in the watershed as shown in figure A.7 and A.8. However, the dominant land use class of the watershed is agricultural land. The dominant soil types are given in figure 6.

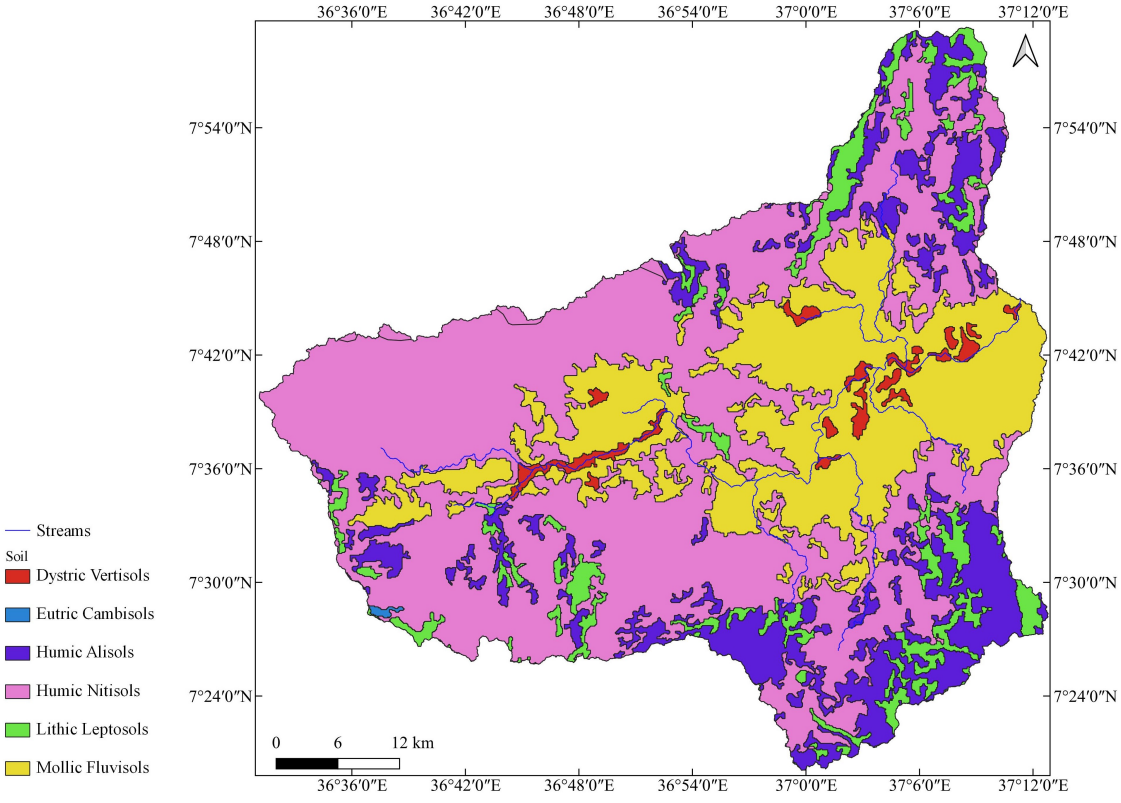

Figure 6: Soil map of the Gilgel Gibe 1 Watershed.

0.2.2. Sediment Rating Curves

A sediment rating curve was required to generate sediment data from the corresponding flow data. Therefore, the sediment data were subject to the

error of the sediment rating curves. Table 1 shows information about suspended sediment and flow data that we collected from the River Basin Authority of Ethiopia.

Table 1: Data type and the length of the record period for each watershed under our consideration.

Name of watershed	Data type	Record period
Hombole and Mojo	Flow	1990–2016
	suspended sediment	1989–2015
Gumera	Flow	2000-2017
	suspended sediment	1990–2017
Gilgel Gibe 1	Flow	2000–2015
	suspended sediment	1990–2017

We considered temporal patterns of weather, land use change, and data-related scenarios to draw a sediment rating curve. Accordingly, the sediment rating curve of each watershed is given in figure 7.

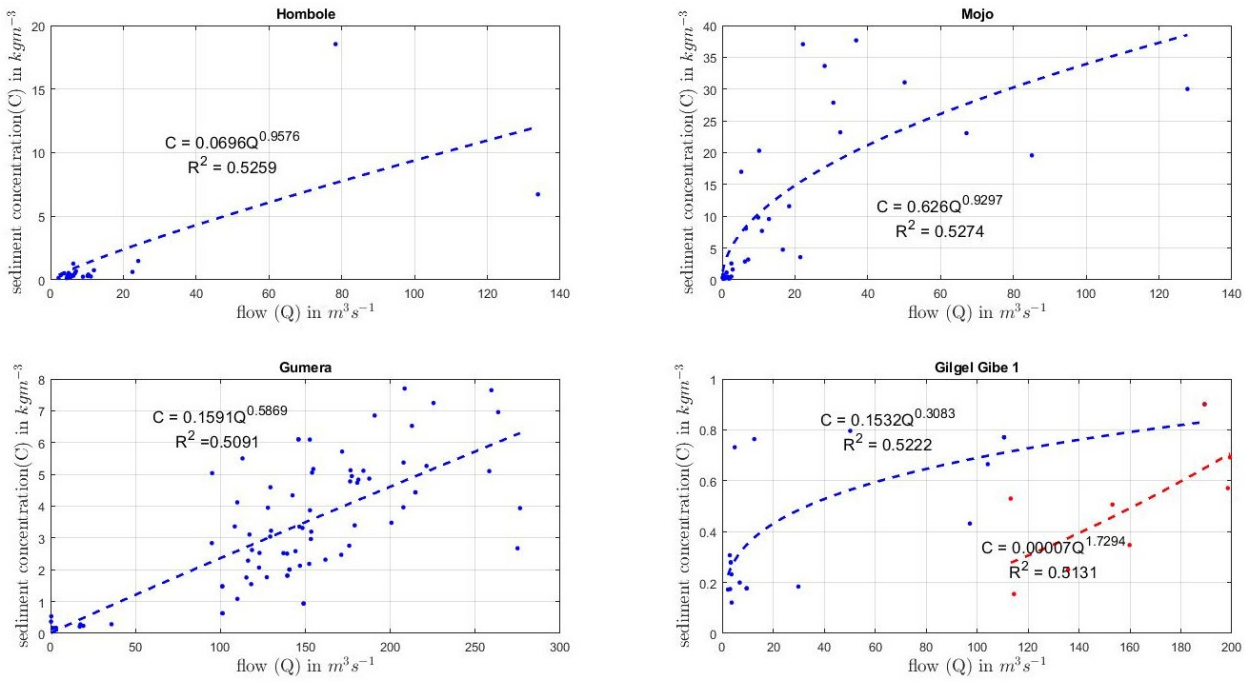

Figure 7: Sediment rating curve for each watershed under our consideration.

0.2.3. Deriving a Soil Loss Equation For Sediment Yield Estimation

As indicated in [Tsige et al., 2022a], the MUSLE was improved based on the underlying physical assumption is that the amount of potential energy of the runoff is proportional to the shear stress for sediment transport from a slope field and the kinetic energy of the runoff at the bottom of the slope field for gully formation. We based on this assumption to derive a soil loss equation. Therefore, let us consider every runoff volume that will begin at every slope height and flows down simultaneously to the bottom of the slope (i.e., the runoff that will start from any point on the entire slope surface due to the uniform

distribution of rainfall on the entire slope field), and a temporal variation of every runoff volume at specific slope height. Let us say the position of first runoff volume, as well as those of the second, third, and so on along the length of the slope are at the slope heights h, h_1, h_2, and so on from the bottom of the slope, respectively; one runoff volume takes over the position of another runoff volume as it flows down to the bottom of the slope.

The total potential energy of the first runoff volume due to its changes in position as it flows down from the height h to the bottom of the slope is equal to E_1.

$$E_1 = \int_0^h \rho v g h dh \tag{1}$$

where ρ is the density in kg/m^3, v is the volume in m^3, g is the acceleration due to gravity in m/s^2, h is the height referring to the position of the runoff volume from the bottom of the slope.

The total runoff volume at a particular point of the slope field is a function of the runoff depth changing with time, where the bottom area of the runoff volume does not change with time. Therefore,

$$v = \int_0^t \left(dA * (i_{rain} - i_{soil})\right) dt \tag{2}$$

$$v = dA \int_0^t \left(i_{rain} - i_{soil}\right) dt \tag{3}$$

where i_{rain} is the rainfall intensity, i_{soil} is the soil infiltration rate

Let

$$Q = \int_0^t \left(i_{rain} - i_{soil}\right) dt \tag{4}$$

Therefore,

$$v = QdA \tag{5}$$

where Q is the runoff depth in m, v is the runoff volume in m^3.

Substitute equation 5 into 1

$$E_1 = dA \int_0^h \rho Q g h dh \tag{6}$$

If the energy of the runoff volume along the length of the slope (i.e., energy per a unit area) is considered, therefore,

$$E_1 = \int_0^h \rho Q g h dh \tag{7}$$

Evaluate integral

$$E_1 = \frac{\rho g Q h^2}{2} \tag{8}$$

The trigonometric relationship between the slope length (h), slope angle (θ), and height (h) is given by

$$h = L sin\theta \tag{9}$$

Substitute equation 9 into 8

$$E_1 = \frac{\rho g Q (L sin\theta)^2}{2} \tag{10}$$

Let us consider the following explanations in the context of runoff energy for sediment yield estimation.

As explained in [Tsige et al., 2022a] to improve the MUSLE, the slope and slope length factors of the MUSLE contribute to the energy of runoff whereas the soil erodibility, cover, and conservation practice factors of the MUSLE contribute to resistance to the runoff. This is because soil conservation practice blocks and at the same time stores the runoff volume up to some level to break

its energy and reduce its velocity, which mainly increases sediment deposition by reducing sediment transport. As there more soil protection works are in a field, more dissipation of the energy of the runoff, and less soil loss from the slope area and the bottom of the slope are expected. A soil cover doesn't store the runoff volume but it blocks the runoff to break its energy, which mainly reduces soil erosion. However, the soil cover may play less importance in facilitating sediment deposition. As dense the soil cover or vegetation becomes, more dissipation of energy of the runoff, and less soil loss from the slope area and the bottom of the slope are expected. It is obvious that soil erodibility contributes to the energy dissipation of the runoff. However, its effect on soil erosion and sediment transport should be explained.

As soil becomes more compacted and smooth, less dissipation of the energy of the runoff, and less soil loss from the slope area, but more soil loss is expected from the bottom of the slope due to the concentrated flow. In this case, the fraction of soil shear resistance against the flow is high (i.e., soil erodibility property is low) along the length of the slope. The runoff volume will have high kinetic energy at the bottom of the slope as the potential energy of the runoff converts to the kinetic energy at the bottom of the slope. Due to the high kinetic energy at the bottom of the slope, the runoff will have high speed and momentum to scour the soil surface and leads to the gully formation at the bottom of the slope. As soil becomes more loose or rough, more dissipation of the energy of the runoff, more soil loss from the upper parts of the slope area, less sediment transport or more sediment deposition, and less soil loss from the bottom of the slope are expected. This is because the runoff loses its most of energy at the upper part of the slope. In this case, the fraction of soil shear resistance against the runoff is low (i.e., its erodibility property is high)

along the length of the slope. Based on this explanations, if a fraction of soil shear resistance (S_r) against the runoff is zero, then its soil erodibility factor (K) is one. Therefore,

$$S_r = 1 - K \tag{11}$$

According to this equation, when we say a given soil is difficult to erode or transport, we mean that its erodibility property is low or it has high shear resistance against the runoff, which is true.

As slope of the field increases, the energy of the runoff increase, and more soil erosion is expected. As the slope length decreases, obstacles or friction resistance against the runoff decreases, and more erosion due to the energy of the runoff is expected. As the slope length increases, the energy of the runoff decreases as resistance against flow increases along the length of the slope, and its shear force decreases. Therefore, sediment deposition is expected at the lower parts of the slope. Based on this explanation, a coefficient of the energy dissipation should be taken into account for the energy loss of the runoff volume due to the length of the slope, for sediment yield estimation.

Equation 10 shows the total potential energy of the first runoff. Based on the above explanations if the energy loss due to friction is taken into account, the available total energy of the first runoff volume is equal to $\triangle E_1$.

$$\triangle E_1 = \frac{\rho g Q (L sin\theta)^2 (1 - K) C P L_{f1}}{2} \tag{12}$$

where L_{f1} is the coefficient of the energy dissipation due to the length of the slope

Work done by the first runoff volume is equal to W_1

$$W_1 = F_1 * L \tag{13}$$

where F_1 is the force due to the runoff volume, and L is the slope length

The first runoff volume has energy available $\triangle E_1$, therefore

$$W_1 = \triangle E_1 \tag{14}$$

Substitute equation 14 into 13

$$\triangle E_1 = F_1 L \tag{15}$$

Rearrange equation 15

$$F_1 = \frac{\triangle E_1}{L} \tag{16}$$

Substitute equation 12 into 16

$$F_1 = \frac{\rho g Q (L sin\theta)^2 (1 - K) C P L_{f1}}{2L} \tag{17}$$

Simplify equation 17

$$F_1 = \frac{\rho g Q (L sin^2\theta)(1 - K) C P L_{f1}}{2} \tag{18}$$

Let us now consider second runoff volume. The total potential energy of the second runoff volume due to its changes in position as it flows down from the height h_1 (let us say just immediately after the first runoff volume) to the

bottom of the slope is equal to E_2.

$$E_2 = \int_0^{h_1} \rho v g h dh \tag{19}$$

Substitute equation 5 into 19

$$E_2 = dA \int_0^{h_1} \rho Q g h dh \tag{20}$$

If the energy of the runoff volume along the length of the slope (i.e., energy per a unit area) is considered, therefore,

(21)

Evaluate integral

$$E_2 = \frac{\rho g Q h_1^2}{2} \tag{22}$$

The trigonometric relationship between the slope length (L_1), slope angle (θ), and height (h_1) is given by

$$h_1 = L_1 sin\theta \tag{23}$$

Substitute equation 23 into 22

$$E_2 = \frac{\rho g Q (L_1 sin\theta)^2}{2} \tag{24}$$

Equation 24 shows the total potential energy of the second runoff volume. If the energy loss due to friction is taken into account, the available total energy of the second runoff volume is equal to $\triangle E_2$.

$$\triangle E_2 = \frac{\rho g Q (L_1 sin\theta)^2 (1-K) C P L_{f2}}{2} \tag{25}$$

Work done by the second runoff volume is given by

$$W_2 = F_2 * L_1 \tag{26}$$

The second runoff volume has energy available $\triangle E_2$, therefore

$$W_2 = \triangle E_2 \tag{27}$$

Substitute equation 27 into 26

$$\triangle E_2 = F_2 L_1 \tag{28}$$

Rearrange equation 28

$$F_2 = \frac{\triangle E_2}{L_1} \tag{29}$$

Substitute equation 25 into 29

$$F_2 = \frac{\rho g Q (L_1 sin\theta)^2 (1-K) C P L_{f2}}{2L_1} \tag{30}$$

Simplify equation 30

$$F_2 = \frac{\rho g Q (L_1 sin^2\theta)(1-K) C P L_{f2}}{2} \tag{31}$$

Let us now consider the third runoff volume. The total potential energy of the third runoff volume due to its changes in position as it flows down from the height h_2 (let us say just immediately after the second runoff volume) to the bottom of the slope is equal to E_3, and so on.

$$E_3 = \int_0^{h_2} \rho v g h dh \tag{32}$$

Substitute equation 5 into 32

$$E_3 = dA \int_0^{h_2} \rho Q g h dh \tag{33}$$

If the energy of the runoff volume along the length of the slope (i.e., energy per a unit area) is considered, therefore,

$$E_3 = \int_0^{h_2} \rho Q g h dh \tag{34}$$

Evaluate integral

$$E_3 = \frac{\rho g Q h_2^2}{2} \tag{35}$$

The trigonometric relationship between the slope length (L_2), slope angle (θ), and height (h_2) is given by

$$h_2 = L_2 sin\theta \tag{36}$$

Substitute equation 36 into 35

$$E_3 = \frac{\rho g Q (L_2 sin\theta)^2}{2} \tag{37}$$

Equation 37 shows the total potential energy of the third runoff volume. If the energy loss due to friction is taken into account, the available total energy of the third runoff volume is equal to $\triangle E_3$.

$$\triangle E_3 = \frac{\rho g Q (L_2 sin\theta)^2 (1 - K) C P L_{f3}}{2} \tag{38}$$

Work done by the third runoff volume is given by

$$W_3 = F_3 * L_2 \tag{39}$$

The third runoff volume has energy available $\triangle E_3$, therefore,

$$W_3 = \triangle E_3 \tag{40}$$

Substitute equation 40 into 39

$$\triangle E_3 = F_3 L_2 \tag{41}$$

Rearrange equation 41

$$F_3 = \frac{\triangle E_3}{L_2} \tag{42}$$

Substitute equation 38 into 42

$$F_3 = \frac{\rho g Q (L_2 sin\theta)^2 (1-K) C P L_{f3}}{2 L_2} \tag{43}$$

Simplify equation 43

$$F_3 = \frac{\rho g Q (L_2 sin^2\theta)(1-K) C P L_{f3}}{2} \tag{44}$$

Therefore, determine the sum of all runoff forces

$$F = F_1 + F_2 + F_3 ... + F_n \tag{45}$$

Substitute equation 18, 31, 44, and so on into 45.

$$F = \frac{\rho g Q (L sin^2\theta)(1-K) C P L_{f1}}{2} + \frac{\rho g Q (L_1 sin^2\theta)(1-K) C P L_{f2}}{2} + \frac{\rho g Q (L_2 sin^2\theta)(1-K) C P L_{f3}}{2} + ... + F_n \tag{46}$$

where L_1 and L_2 are the lengths of the slope corresponding to the heights

of the slope h_1 and h_2 respectively provided that h_1 and h_2 are the heights of the slope just immediately after heights h and h_1 respectively, and so on. Therefore, equation 46 is written as

$$F = \int_0^L \frac{\rho g Q (L sin^2\theta)(1-K) C P L_f}{2} dL \tag{47}$$

Simplify equation 47

$$F = \frac{\rho g Q sin^2\theta * (1-K) * CP \int_0^L (L * L_f) dL}{2} \tag{48}$$

Next, we define soil shear resistance (shear force) which acts against the runoff direction parallel to the slope length.

Soil shear resistance which acts at slope height h_1 parallel to the length of the slope is equal to f_1

$$f_1 = m_1 g cos\theta \tag{49}$$

where m_1 is the mass of soil, g is the acceleration due to gravity

Soil shear resistance which acts at slope height h_2 parallel to the length of the slope is equal to f_2

$$f_2 = m_2 g cos\theta \tag{50}$$

Soil shear resistance which acts at slope height h_3 parallel to the length of the slope is equal to f_3

$$f_3 = m_3 g cos\theta \tag{51}$$

Soil shear resistance which acts at slope height h_n parallel to the length of the slope is equal to f_n

$$f_n = m_n g cos\theta \tag{52}$$

Sum all shear resistances (shear forces) which act against the runoff direction is equal to F_s

$$F_s = F_1 + F_2 + F_3 + ... + F_n \tag{53}$$

Substitute equations 49 – 52, and so on into equation 54

$$F_s = m_1 gcos\theta + m_2 gcos\theta + m_3 gcos\theta + ... + m_n gcos\theta \tag{54}$$

Simplify equation 54

$$F_s = mgcos\theta \tag{55}$$

where m is the total mass of sediment

At equilibrium, where sediment deposition takes place or sediment sinks into a channel at the end of the slope field, the runoff force (F) is taken to be counterbalanced by the soil shear resistance (F_s).

$$F = F_s \tag{56}$$

Substitute equations 48 and 55 into 56

$$\frac{\rho g Q sin^2\theta * (1-K) * CP \int_0^L (L * L_f) dL}{2} = mgcos\theta \tag{57}$$

Rearrange equation 57

$$m = \frac{\rho Q (1-K) CP sin^2\theta}{2cos\theta} \int_0^L (L * L_f) dL \tag{58}$$

Next, let us consider the rainfall impact energy for soil erosion. If the free fall velocity (terminal velocity) of a raindrop is considered, then the kinetic energy

(KE) of the raindrop that causes soil erosion on the slope field is given by

$$KE = \frac{1}{2}mv^2cos\theta \tag{59}$$

where m is the mass of the raindrop, and u is the terminal velocity of the raindrop

But $m = \rho * V$, therefore

$$KE = \frac{1}{2}\rho V u^2 cos\theta \tag{60}$$

where ρ is the density of the raindrop, and V is the volume of the raindrop

The total kinetic energy (KE_{total}) of the raindrops on the entire slope field is given by

$$KE_{total} = \frac{1}{2}\rho V_t u^2 cos\theta \tag{61}$$

where V_t is the total volume of the raindrop

Let us assume that the raindrop is uniformly distributed over the entire slope field, therefore, the total volume of the raindrops (V_t) is given by

$$V_t = Ah \tag{62}$$

where A is the area of the slope field, and h is the height of the raindrop

Substitute equation 62 into 61

$$KE_{total} = \frac{1}{2}\rho A h u^2 cos\theta \tag{63}$$

where KE_{total} is the total kinetic energy of the raindrops

The area of the slope field is given by

$$A = Lw \tag{64}$$

where L is the length of the slope field, and w is the width of the slope field

Substitute equation 64 into 63

$$KE_{total} = \frac{1}{2}\rho Lwhu^2 cos\theta \tag{65}$$

Consider equation 65

The total kinetic energy per a unit width of the slope is given by

$$KE_{total} = \frac{1}{2}\rho Lhu^2 cos\theta \tag{66}$$

The total amount of soil loss (m) is proportional to the total kinetic energy of the raindrops, soil resistance against the rainfall impact, and soil cover. The soil resistance against the rainfall impact can be taken as the soil erodibility factor of the USLE. Since the soil cover reduces soil erosion by reducing the raindrop impact energy, it can be taken as the cover factor of the USLE. Since the soil conservation practice factor has no role in reducing the rainfall impact energy, we will not consider it in the context of the rainfall energy for soil erosion. Therefore,

$$m \sim KE_{total} * KC \tag{67}$$

Substitute equation 66 into 67

$$m \sim \frac{1}{2}\rho Lhu^2 cos\theta * KC \tag{68}$$

where K is the soil erodibility factor, and C is the cover factor of the USLE Equation 58 is based on runoff energy whereas equation 68 is based on rainfall energy for estimation of the amount of soil loss from a slope field. As runoff is directly proportional to rainfall, the amount of soil loss due to the runoff is directly proportional to the amount of soil loss due to the rainfall. Therefore, correlate equation 58 and 68.

$$\frac{\rho Q(1-K)CPsin^2\theta}{2cos\theta}\int_0^L (L*L_f)dL \sim \frac{1}{2}\rho Lhu^2cos\theta * KC \tag{69}$$

Rearrange equation 69

$$\int_0^L (L*L_f)dL \sim \frac{hu^2Kcos^2\theta}{Q(1-K)Psin^2\theta}L \tag{70}$$

Equation 70 can be written as

$$\int_0^L (L*L_f)dL \sim \int_0^L \frac{hu^2Kcos^2\theta}{Q(1-K)Psin^2\theta}dL \tag{71}$$

Simplify equation 71

$$L*L_f \sim \frac{hu^2Kcos^2\theta}{Q(1-K)Psin^2\theta} \tag{72}$$

Rearrange equation 72

$$L_f \sim \frac{hu^2Kcos^2\theta}{Q(1-K)Psin^2\theta} * \frac{1}{L} \tag{73}$$

Since the effect of the slope length on soil erosion can be seen while keeping other variables constant. Therefore,

$$L_o = \frac{hu^2Kcos^2\theta}{Q(1-K)Psin^2\theta} \tag{74}$$

where L_o is the constant

Substitute equation 74 into 73

$$L_f \sim \frac{L_o}{L} \tag{75}$$

By defining the proportionality constant c and v

$$L_f = c\frac{L_o}{L^v} \tag{76}$$

We expect sediment transport by a runoff volume if $0 < L_f \leq 1$. As a slope length increases, L_f decreases to zero. As a slope length becomes smaller and smaller, L_f approaches one. Since L_f is inversely proportional to L, a value of v should be a positive value. If $cL_o > 1$ and $L < 1$, there is no a positive value of v such that $0 < L_f \leq 1$. For a given value of cL_o, there is a possible value of v such that $0 < L_f \leq 1$ if $L \geq 1$. Therefore, the minimum slope length is defined to be 1m (i.e., $L \geq 1m$) from which soil erosion and sediment transport take place.

Let $v = 1$

$$L_f = c\frac{L_o}{L} \tag{77}$$

Substitute equation 77 into 58

$$m \sim \frac{\rho Q(1-K)CPsin^2\theta}{2cos\theta} \int_0^L (L * c\frac{L_o}{L})dL \tag{78}$$

Evaluate integral

$$m \sim \frac{\rho Q(1-K)CPsin^2\theta}{2cos\theta} L * cL_o \tag{79}$$

For a particular field with slope angle and length, soil cover, soil erodibility, and conservation practice can be controlled. Runoff due to rainfall determines hydro-climatic conditions of the field, and it independently affects soil loss from the field. Therefore, by defining the proportionality constants a_o and b

$$m = \frac{a_o \rho Q^b (1-K) C P sin^2\theta}{2cos\theta} L * cL_o \tag{80}$$

Since a_0, ρ, c, L_0 are all constants, let $a = \frac{1}{2} a_o \rho c L_o$. Therefore, equation 80 is given as

$$m = \frac{a Q^b (1-K) C P sin^2\theta}{cos\theta} L \tag{81}$$

We call equation 81 the Soil Loss Equation for Sediment Yield Estimation (SLESYE).

0.2.4. Evaluating the SLESYE

Just like the improved MUSLE which does not consider the peak runoff rate [Tsige et al., 2022a], the SLESYE is also based on runoff (Q), soil erodibility (K), slope steepness(θ), slope length (L), cover factor (C), and conservation practice factor (P). Therefore, we evaluate the SLESYE in the same way as the MUSLE or improved MUSLE. Thus, we evaluate the SLESYE by considering annual simulation time step and its appropriate calibration parameters.

The annual simulation time step enables taking into account gully erosion, gradual soil erosion processes and gradual changing activities like the cyclic behavior of agricultural activities, conservation practice, flood protection activities, plant growth, and harvest with respect to the rainfall pattern and extreme events in a 1-year full cycle.

Compared with the cover factor, conservation practice factor, and coefficient of the SLESYE, the individual effect of the exponent and soil erodibility factor of the SLESYE is reflected during calibration of the sediment yield rather than their product effect. Therefore, estimating the exponent and soil erodibility factor of the SLESYE through calibration is more feasible than through other parameters of the SLESYE. For a given uniform watershed, the topographic factor does not change with time (i.e., it has a constant effect), and the effect of the topographic factor can be seen when the SLESYE is applied at different watersheds. In general, runoff and the sediment data reflect the hydroclimatic conditions of a particular area, which independently affect the overall calibration process. Our main task is to estimate the best exponent of the SLESYE by applying the model at different watersheds. For the sake of calibration procedure, the main variables of the SLESYE which directly affect soil erosion process such as cover, conservation practice and soil erodibility are estimated based on the past experiences from the literature and comparative approaches, whereas the parameters which do not directly affect the soil erosion process or which have no direct physical meaning (i.e., coefficient and exponent) are estimated through calibration. For the sake of comparison purposes, we test the SLESYE at four watersheds of Ethiopia where the MUSLE and improved MUSLE were tested before by following a similar evaluation procedure.

Based on the above explanations, we estimate the soil erodibility, soil cover, and conservation practice factors in the same ways as the MUSLE or improved MUSLE. The procedures to estimate each factor are given in [Tsige et al., 2022a].

For the slope angle and slope length, the SWAT+ was used to define as

many hydrologic response units (hrus) as possible to consider an areal distribution of the slope steepness and slope length. In the TxtInOut folder of SWAT+, the area and topography information of each hru were stored in the hru.con and topography.hyd files, respectively. These files were exported to an Excel spreadsheet for analysis.

For a chosen value of the exponent b, the best fit corresponding value of coefficient a was estimated through calibration. The selection of the best exponent was performed after calibration of the observed and simulated sediment. During calibration, the Nash–Sutcliffe efficiency corresponds to each exponent b and coefficient a are evaluated, and graphs of exponent b versus the Nash–Sutcliffe efficiency and coefficient a versus exponent b are drawn for each watershed.

We used observed runoff volume to predict sediment load, and we used observed suspended sediment load to calibrate the model. Thus, figure 8 shows sample graphs of the calibrated sediment, and figure 9 shows graphs of exponent b versus the Nash-Sutcliffe efficiency as well as coefficient a versus exponent b.

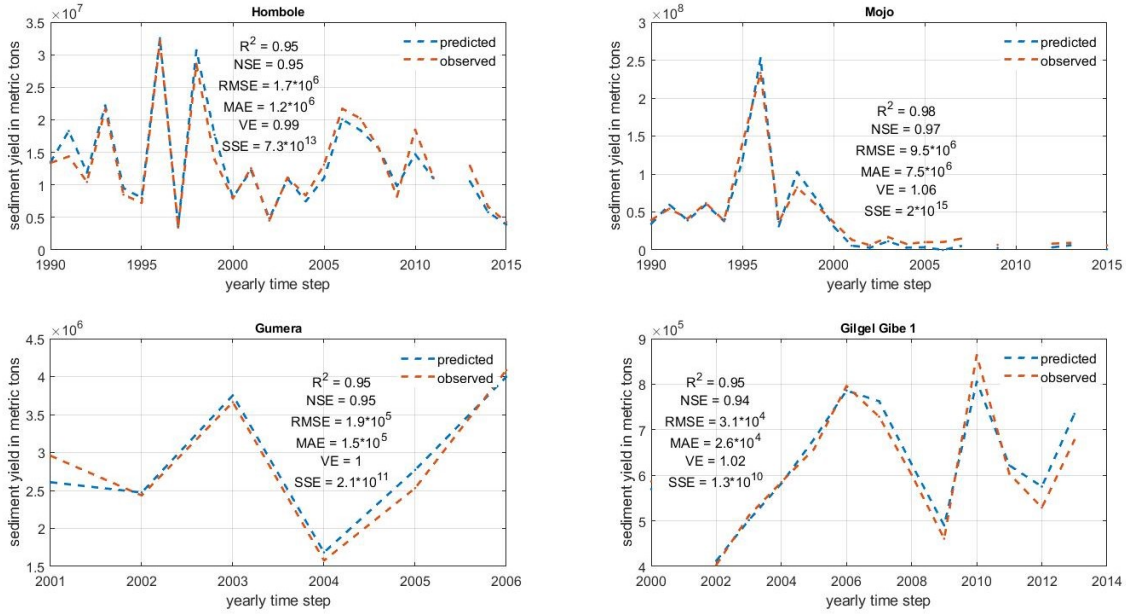

Figure 8: Sample graphs of observed and predicted sediment for all four watersheds under our consideration. The correlation between the graphs is measured using the Nash–Sutcliffe efficiency (NSE), coefficient of determination (R^2), root mean square error (RMSE), mean average error (MAE), volume error (VE), and sum of square error (SSE).

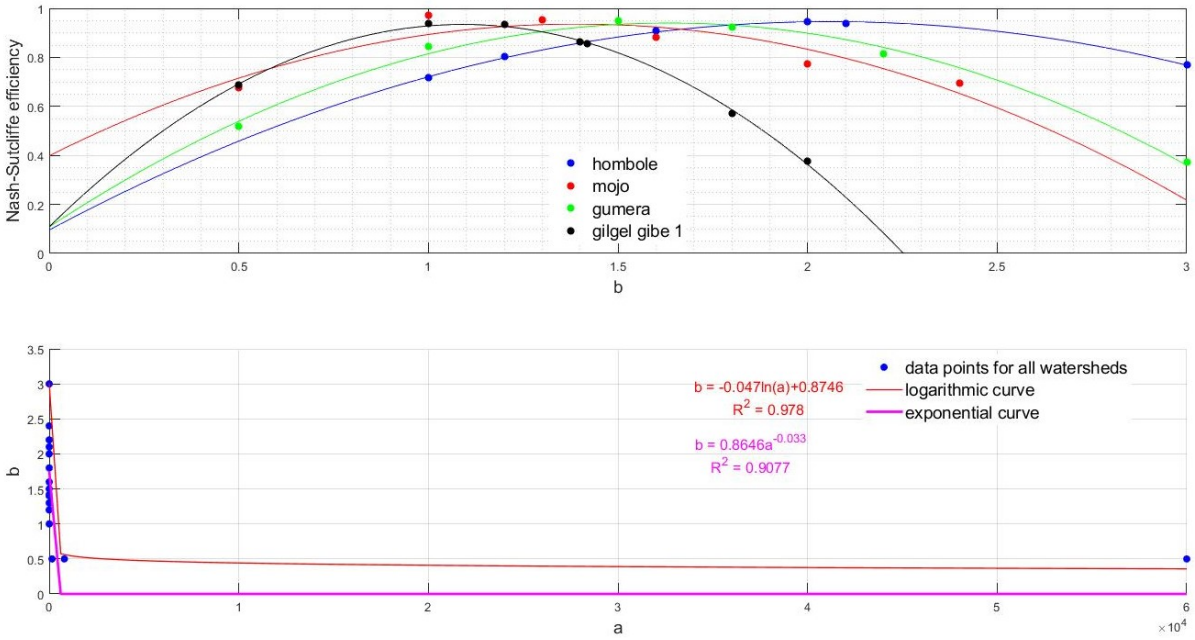

Figure 9: The relationship between the exponent of the SLESYE and the Nash-Sutcliffe efficiency as well as the coefficient of the SLESYE versus its exponent.

0.3. Results

We called equation 81 the SLESYE. From figure 9, if one watershed was considered, the exponent of the SLESYE which resulted in the maximum Nash-Sutcliffe efficiency was taken, but if two or more watersheds were considered, the exponent of the SLESYE which resulted in the minimum Nash-Sutcliffe efficiency was taken. Accordingly, the best actual exponent of the PBSLE was 1.4, which resulted in a Nash-Sutcliffe efficiency of 0.86.

For watersheds under our consideration, as the relationship between the coefficient and exponent of the SLESYE approaches to power or logarithmic function; the relationship between the exponent and the Nash-Sutcliffe effi-

ciency approaches to a quadratic function (refer to figure 9).

0.4. Discussion

In the SLESYE, the slope steepness factor (S) is given by

$$S = \frac{\sin^2 \theta}{\cos \theta} \tag{82}$$

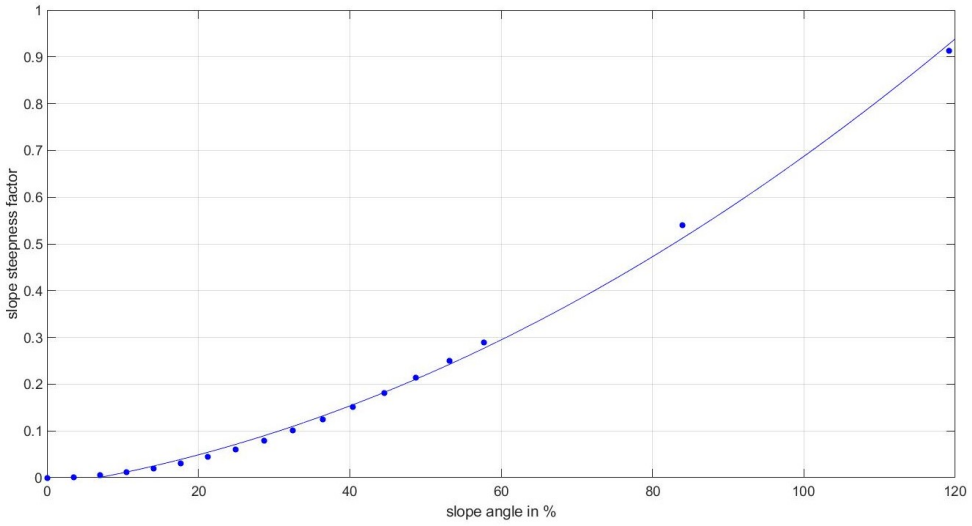

Figure 10: The relationship between slope angle and slope steepness factor of the SLESYE

As slope angle increases slope steepness factor increases. As the slope steepness factor increases more soil erosion and sediment transport are expected. From figure 10, there is a direct relationship between slope angle and slope steepness factor of the SLESYE. Therefore, the derived equation of the slope steepness factor is appropriate.

A similarity between the SLESYE and MUSLE is that the runoff volume or depth, soil cover factor, soil conservation practice factor, slope steepness factor, and slope length are directly proportional to sediment yield from a slope field. A primary difference between the SLESYE and MUSLE is that soil erodibility is directly proportional to the sediment yield in the case of the MUSLE, whereas in the case of the SLESYE the soil erodibility is indirectly proportional to the sediment yield. These two proportionalities can be explained by considering three cases.

a) Case one: how is sediment yield affected if runoff volume is constant in given periods but soil erodibility increases ?

The MUSLE and SLESYE estimate the total sediment load based on the total runoff volume. In the case of the MUSLE, the relationship between an individual runoff volume and soil erodibility on sediment transport is not well defined. The SLESYE was derived while considering the effect of an individual runoff volume and soil erodibility on sediment transport.

For the same runoff volume (i.e., for the same rainfall distribution in given periods), as soil erodibility increases from period to period, the runoff volume gets concentrated with sediment particles. This action reduces sediment transport and facilitates sediment deposition along the length of the slope, which eventually leads to mud concentration at the lower parts of the slope. Therefore, sediment yield at the bottom end of the slope or an outlet of a watershed is expected to decrease as soil erodibility increases. For example, if we consider silt and clay soil, silt soil is easily erodible as compared with clay soil (this is due to cohesive force between soil particles, clay soil has higher cohesive force than silt soil). Therefore, for the same runoff volume, sediment yield is expected to decrease for silt soil due to deposition (one reason for the deposition can be

the settling velocity of soil particles; silt soil settles first as compared with clay soil). Actually, soil erodibility expresses highly erodible soil to non-erodible soil (rocky or paved soil). In the SLESYE, if $K = 1$, it shows mud or high shear stress. In this case, no sediment transport is expected. If $K = 0$, it shows a rocky or paved area. In this case, the cover factor is zero, and therefore, no soil erosion is expected. This shows that soil erosion and sediment transport are expected in the range of these two extremes. In the MUSLE, these two extremes are not clearly defined or the type of soil which has soil erodibility factor one or zero is not clearly defined.

Based on these explanations, the MUSLE does not consider the sediment deposition process, whereas the SLESYE considers the sediment deposition process. Therefore, the SLESYE is more appropriate than the MUSLE.

b) Case two: how is sediment yield affected if runoff volume increases in given periods but soil erodibility is constant ?

For the same soil erodibility, as runoff volume increases from period to period, soil erosion and sediment transport are expected to increase and sediment deposition is expected to decrease due to the scouring power of the runoff volume. In this case, how soil erosion can be increased if soil erodibility is constant?

Since soil erodibility refers to the property of soil which indicates how a given soil is erodible or susceptible to erosion or it refers to the degree of ease in eroding a given soil, it does not tell us the mass of the soil. For example, soil erodibility tells us how easy to erode silt soil compared with clay soil, but it does not directly tell us the mass of silt soil available in a given field. In this context, more runoff volume erodes and caries more silt soil or other type of soil having constant erodibility.

Therefore, based on above explanations, both the MUSLE and the SLESYE hold true.

c) Case three: how is sediment yield affected if both runoff volume and soil erodibility increase simultaneously in given periods ?

Depending on the magnitude of runoff volume and soil erodibility factor, soil erosion and sediment deposition processes are not easy to define. As long as both the MUSLE and the SLESYE are empirical models in nature, the SLESYE is more convenient approach for estimation of sediment yield from a slope field.

0.5. Conclusions

The SLESYE is given by

$$y = aQ^b(1-K)CPL\frac{\sin^2\theta}{\cos\theta} \tag{83}$$

where y is the sediment yield in metric tons, a is the coefficient, b is the exponent, Q is the runoff depth in m, K is the soil erodibility factor, L is the slope length, θ is the angle of slope in degree, $\frac{\sin^2\theta}{\cos\theta}$ is the slope steepness factor (S), C is the soil cover factor, P is the soil conservation practice factor.

The performance of the SLESYE is greater than or equal to 86% for all watersheds under our consideration. Therefore, the performance of the SLESYE was better than the regionalized MUSLE (i.e., the minimum performance was 80%) [Tsige et al., 2022b] or improved MUSLE (i.e. the minimum performance was 84%) [Tsige et al., 2022a]. The theoretical exponent of the SLESYE is determined in the same way as the improved MUSLE [Tsige et al., 2022a]. The

best actual exponent of the SLESYE was 1.4 based on four watersheds under our consideration.

Unlike the MUSLE and improved versions of the MUSLE, the SLESYE explains sediment transport and deposition processes. Therefore, physically speaking, the SLESYE is the most appropriate than the MUSLE and improved versions of the MUSLE. The SLESYE does not consider peak runoff rate, and therefore, it is advantageous to the data-scarce area as the peak runoff rate is not commonly available data. Another advantage of the SLESYE over the MUSLE and improved versions of the MUSLE is that the individual effect of the soil erodibility factor is reflected during the calibration of sediment yield rather than its product effect. Therefore, in the case of the SLESYE, the soil erodibility factor can be determined through calibration for a particular area. If we include the peak runoff rate in the SLESYE, the physical meaning for sediment estimation is still appropriate, we also recommend including the peak runoff rate in the SLESYE and testing its performance if the peak runoff data are available.

Like the MUSLE and improved versions of the MUSLE, the SLESYE does not consider channel erosion, mudflow, and massive land movement due to landslides or slumps. We can not exactly tell whether the MUSLE considers gully erosion or not, there is no indication to say gully erosion is considered in the SLESYE. This is because runoff concentration can lead to gully formation.

Funding

This research was funded by the German Academic Exchange Service and Universität der Bundeswehr München.

Disclosure statement

The authors have no relevant financial or non-financial interests to disclose.

Data availability

The data are available from the corresponding author upon reasonable request. Climate data (from 1986 to 2020 for all watersheds) are from the National Meteorology Agency of Ethiopia. Flow data (from 1990 to 2016 for Hombole and Mojo watersheds; from 2000 to 2017 for Gumera watershed; from 2000 to 2015 for Gilgel Gibe 1 watershed) and sediment data (from 1989 to 2015 for Hombole and Mojo watersheds; from 1990 to 2017 for Gumera and Gilgel Gibe 1 watersheds) are from the River Basin Authority of Ethiopia. Digital Elevation Models are from the US Geological Survey. Land use and soil data sources are available at https://www.preprints.org/manuscript/202202.0163/v1

Bibliography

V. Bagarello, V. Ferro, and V. Pampalone. A new version of the usle-mm for predicting bare plot soil loss at the sparacia (south italy) experimental site. *HYDROLOGICAL PROCESSES*, 2015. doi: 10.1002/hyp.10486.

V. Bagarello, C. D. Stefano, V. Ferro, and V. Pampalone. Comparing theoretically supported rainfall-runoff erosivity factors at the sparacia (south italy) experimental site. *Hydrological Processes*, 2018. doi: 10.1002/hyp.11432.

L. Baoyuan, Z. Keli, and X. Yun. An empirical soil loss equation. *Proceedings*

of 12th International Soil Conservation Organization Conference, Tsinghua University Press, Beijing, pages 21–25, 2002.

Guangyao Gao, Yue Liang, Jianbo Liu, David Dunkerley, and Bojie Fu. A modified rusle model to simulate soil erosion under different ecological restoration types in the loess hilly area. *International Soil and Water Conservation Research*, 12(2):258–266, 2024. ISSN 2095-6339. doi: https://doi.org/10.1016/j.iswcr.2023.08.007. URL https://www.sciencedirect.com/science/article/pii/S2095633923000692.

P. I. A. Kinnell and L. M. Risse. Usle-m: Empirical modeting rainfall erosion through runoff and sediment concentration. *Soil Science Society of AnericaJournal*, 62(6), 1998. doi: 10.2136/sssaj1998.03615995006200060026x.

K.G. Renard, G.R. Foster, G.A Weesies, D.K. McCool, and D.C. Yoder. *Predicting Soil Erosion by Water: A Guide to Conservation Planning with the Revised Universal Soil Loss Equation.* USDA, Agriculture Handbook, No 703, 404pp., 1997.

S. H. R. Sadeghi, L. Gholami, A. K. Darvishan, and P. Saeidi. A review of the application of the MUSLE model worldwide. *Hydrological Sciences Journal*, 59:365–375, 2014. ISSN 2150-3435. doi: 10.1080/02626667.2013.866239.

Wenhai Shi, Tiantian Chen, Jiawen Yang, Qianfang Lou, and Ming Liu. An improved musle model incorporating the estimated runoff and peak discharge predicted sediment yield at the watershed scale on the chinese loess plateau. *Journal of Hydrology*, 614:128598, 2022. ISSN 0022-1694. doi: https://doi.org/10.1016/j.jhydrol.2022.128598. URL https://www.sciencedirect.com/science/article/pii/S0022169422011684.

Manaye Getu Tsige, Andreas Malcherek, and Yilma Seleshi. Improving the modified universal soil loss equation by physical interpretation of its factors. *Water*, 14(9), 2022a. ISSN 2073-4441. doi: 10.3390/w14091450. URL https://www.mdpi.com/2073-4441/14/9/1450.

Manaye Getu Tsige, Andreas Malcherek, and Yilma Seleshi. Estimating the best exponent and the best combination of the exponent and topographic factor of the modified universal soil loss equation under the hydro-climatic conditions of ethiopia. *Water*, 14(9), 2022b. ISSN 2073-4441. doi: 10.3390/w14091501. URL https://www.mdpi.com/2073-4441/14/9/1501.

H.D. Williams, J.R; Berndt. Sediment yield prediction based on watershed hydrology. *ASAE*, pages 1100–1104, 1977. doi: 10.13031/2013.35710.

J. R. Williams. Sediment routing for agricultural watersheds. *Water Resources Bulletin*, 11:965–974, 1975.

W. H. Wischmeier and D. Smith. *Predicting Rainfall Erosion Losses: A Guide to Conservation Planning*. United States Department of Agriculture, 1978.

Appendix

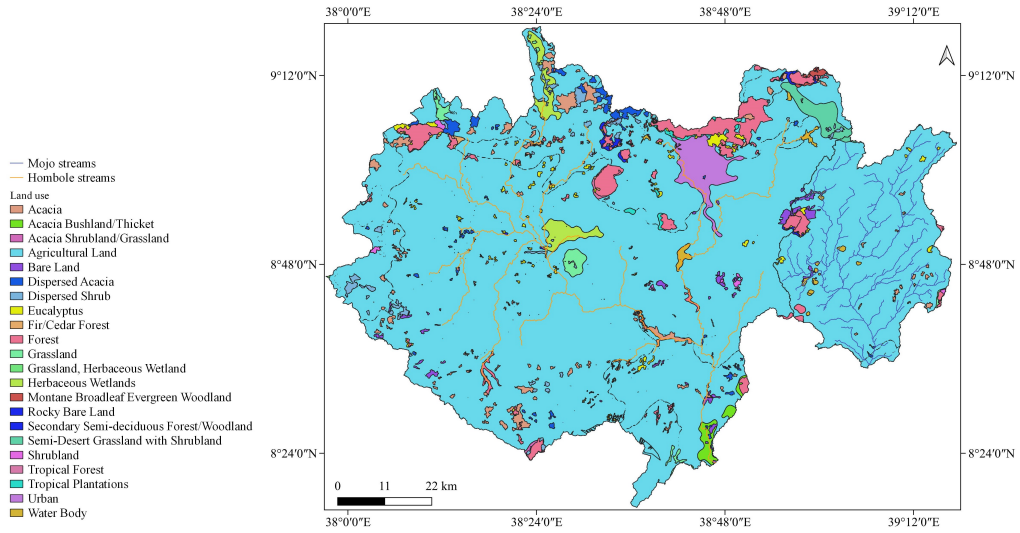

Figure A.1: Land use map of the Hombole and Mojo Watersheds from 1989 to 2000.

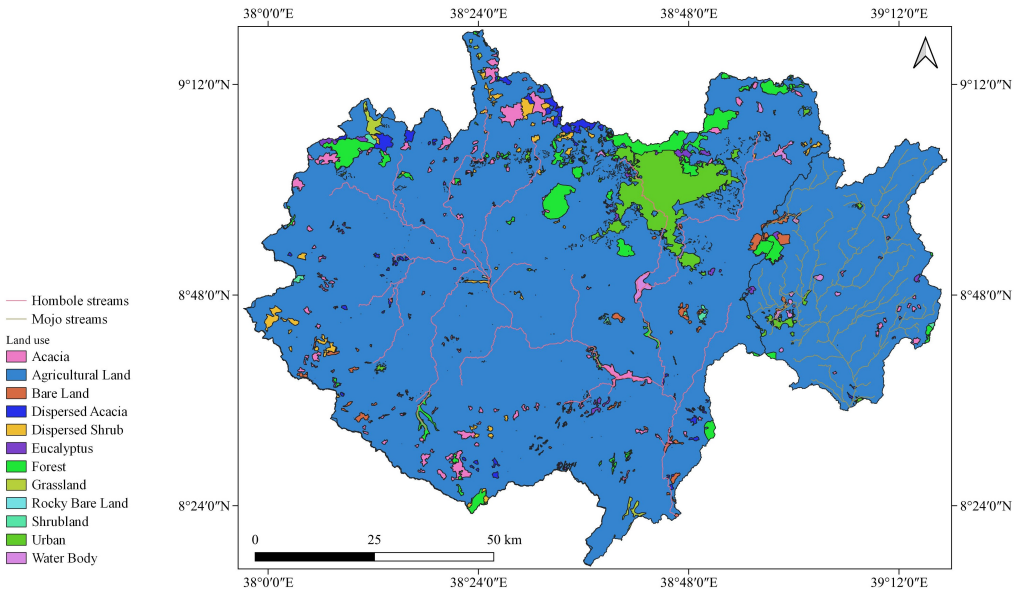

Figure A.2: Land use map of the Hombole and Mojo Watersheds from 2001 to 2008.

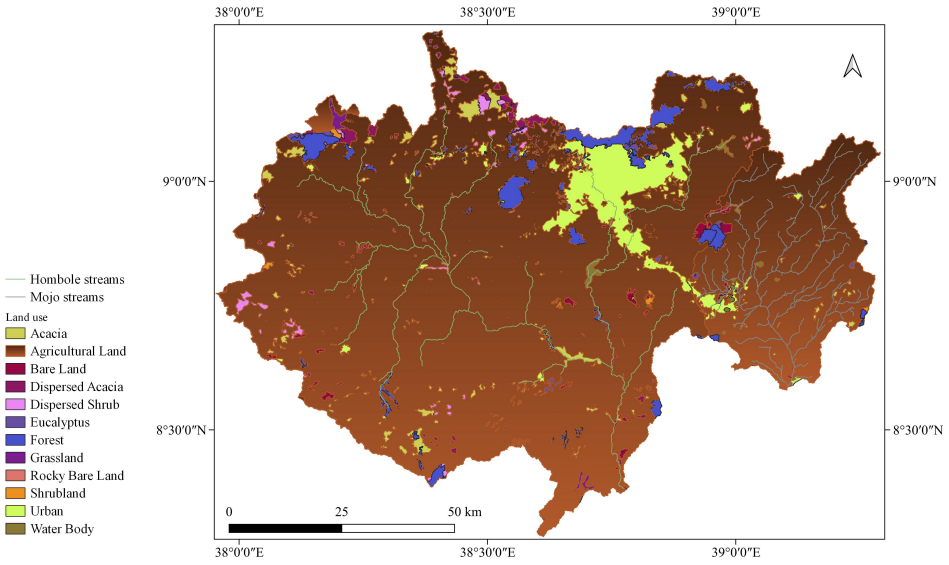

Figure A.3: Land use map of the Hombole and Mojo Watersheds from 2009 to 2012.

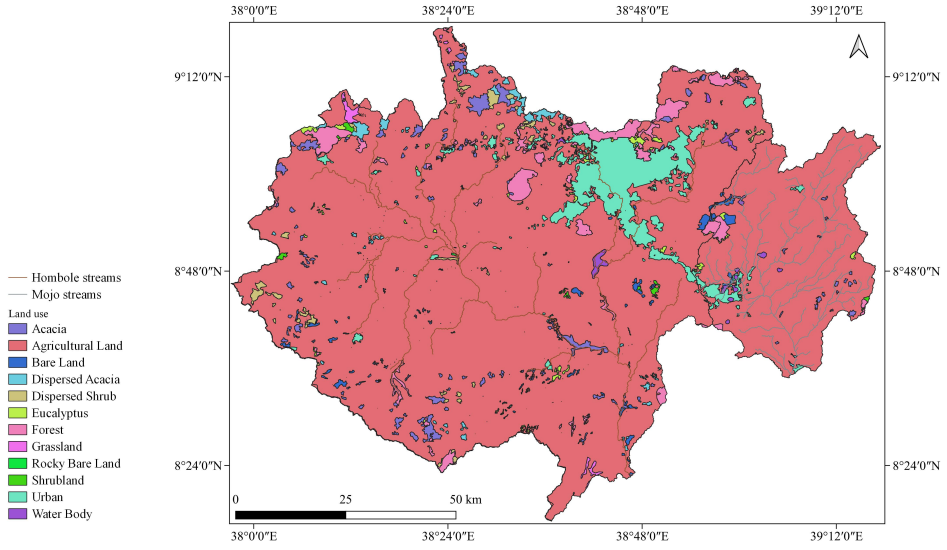

Figure A.4: Land use map of the Hombole and Mojo Watersheds from 2013 to 2015.

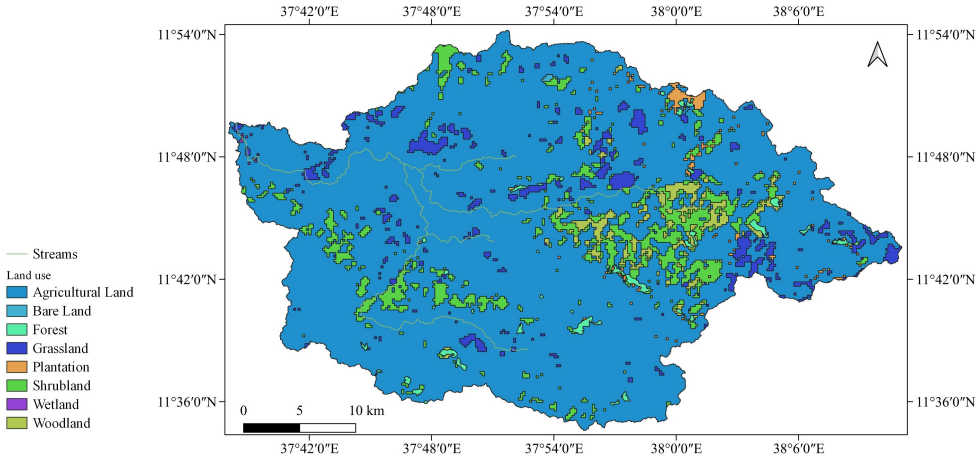

Figure A.5: Land use map of the Gumera Watershed from 1989 to 2009.

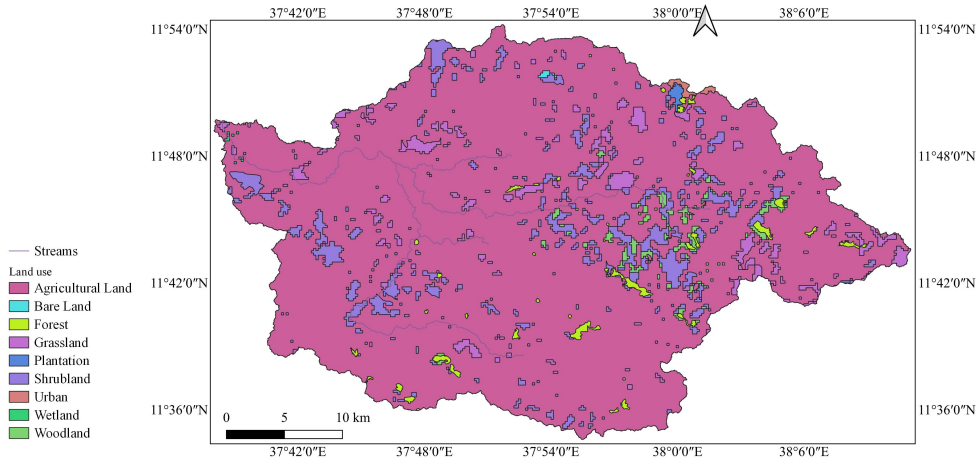

Figure A.6: Land use map of the Gumera Watershed from 2010 to 2015.

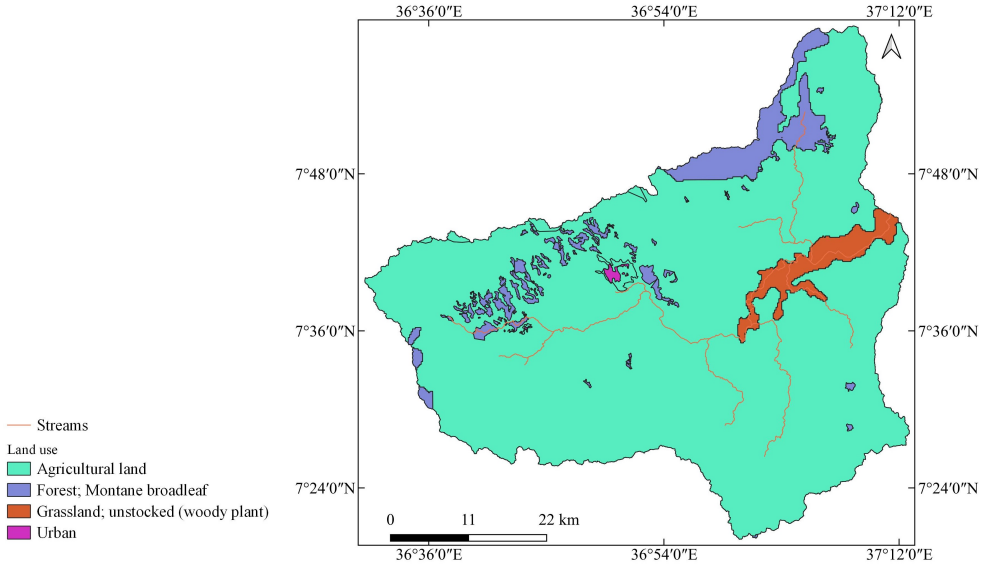

Figure A.7: Land use map of the Gilgel Gibe 1 Watershed from 1989 to 2009.

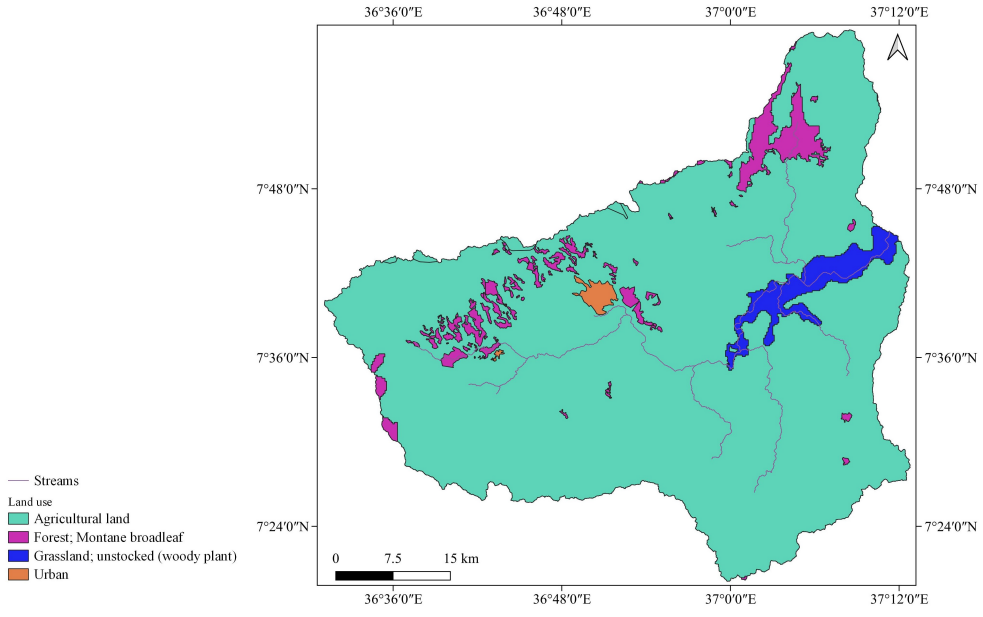

Figure A.8: Land use map of the Gilgel Gibe 1 Watershed from 2010 to 2015.